Testing the dark matter subhalo hypothesis of the gamma-ray source 3FGL J2212.5+0703

Yuan-Peng Wang,[1,2] Kai-Kai Duan,[1,2] Peng-Xiong Ma,[1,2] Yun-Feng Liang,[1,2,*] Zhao-Qiang Shen,[1,2,†] Shang Li,[1,2,‡] Chuan Yue,[1,2] Qiang Yuan,[1] Jing-Jing Zang,[1] Yi-Zhong Fan,[1,§] and Jin Chang[1]

[1]*Key Laboratory of Dark Matter and Space Astronomy, Purple Mountain Observatory, Chinese Academy of Sciences, Nanjing 210008, China*

[2]*University of Chinese Academy of Sciences, Beijing 100012, China*

(Received 7 October 2016; published 2 December 2016)

N-body simulations predict that galaxies at the Milky Way scale host a large number of dark matter (DM) subhalos. Some of these subhalos, if they are massive enough or close enough to the Earth, might be detectable in γ rays due to the DM annihilation. 3FGL J2212.5+0703, an unidentified gamma-ray source, has been suggested to be the counterpart candidate of a DM subhalo by Bertoni *et al.* In this work we analyze the Fermi-LAT Pass 8 data of 3FGL J2212.5+0703 to independently test the DM subhalo hypothesis of this source. In order to suppress the possible contamination from two nearby very bright blazars, we just take into account the front-converting gamma rays which have better angular resolutions than that of the back-converting photons. In addition to the spatial distribution analysis, we have extended the spectrum analysis down to the energies of ∼100 MeV, and thoroughly examined the variability of the emission during the past 8 years. We confirm that 3FGL J2212.5+0703 is a steady and spatially extended gamma-ray emitter at a high confidence level. The spectrum is well consistent with that expected from DM annihilation into $b\bar{b}$. The introduction of a phenomenological LogParabola spectrum just improves the fit slightly. All these results suggest that 3FGL J2212.5+0703 could be indicative of a DM subhalo.

DOI: 10.1103/PhysRevD.94.123002

I. INTRODUCTION

Compelling evidence indicates that dark matter (DM) plays a significant role in many gravitational phenomena such as the galactic rotation curves, the galaxy cluster dynamics, and the cosmic microwave background [1–3]. The latest measurements suggest that DM constitutes 84.3% of the matter density in the current Universe [4]. Abundant as DM is, its particle physics nature remains unknown. Various well-motivated DM candidates have been proposed in the literature and the leading candidate is the weakly interacting massive particles (WIMPs) [1–3,5–7]. WIMPs may annihilate or decay and finally produce stable high-energy particle pairs, including, for example, electrons/positrons, protons/antiprotons, neutrinos/antineutrinos, and gamma rays. These stable particles contribute to the cosmic radiation. The identification of these DM-originated particles in the gamma-ray and cosmic ray data is the prime goal of dark matter indirect detection. DM induced γ rays are either from the decay or hadronization of the final state particles (i.e., prompt radiation), or from the final state particles interacting with interstellar medium or interstellar radiation field (i.e., secondary radiation). Unlike the charged particles that are deflected by the magnetic fields, gamma rays travel straightforwardly and their morphology traces the distribution of the emitting sources directly. Therefore, the searches for the DM signal in the gamma-ray data, benefited from the spatial correlation with the DM distribution, have attracted wide attention. This is, in particular, the case after the successful launch of the *Fermi Gamma-ray Space Telescope* in June 2008 [7,8]. Great efforts have been made to analyze the Fermi-LAT (Large Area Telescope) data, but no reliable DM signal has been identified so far (see [7] for a recent review).

Among various targets, the Milky Way dwarf spheroidal galaxies (dSphs), dominated by DM and in short of high-energy astrophysical processes, are promising regions to identify the DM signal indirectly. The identification of dSphs in optical, however, is rather challenging due to their low luminosities. Until recently, only 25 dSphs were found by the Sloan Digital Sky Survey (SDSS) [9] and the observations prior to it (see [10] and the references therein). Over the past two years, 23 more dSphs (including candidates) have been discovered due to new optical image surveys [11–18] such as the Dark Energy Survey (DES) [19] and the Pan-STARRS1 3π survey [20], or due to the reanalysis of the SDSS data. Although many analyses have been conducted in search for the γ-ray emission from these dSph sources and candidates [21–37], none of them display

*Corresponding author.
liangyf@pmo.ac.cn
†Corresponding author.
zqshen@pmo.ac.cn
‡Corresponding author.
lishang@pmo.ac.cn
§Corresponding author.
yzfan@pmo.ac.cn

a statistically significant signal (tentative gamma-ray emission signals were reported in Ret II [29,30] and Tuc III [34,37]).

DM subhalos are also promising targets for DM indirect detection. In the standard hierarchical structure formation theory, dark matter particles accumulate to become small halos, and then merge repeatedly to form larger halos. Some of the halos, if survived from the tidal stripping and virialization, become subhalos of the main halo [38,39]. N-body simulations at the scale of the Milky Way show much more subhalos than satellites observed at optical wavelengths [40,41], indicating the majority of them contain little stars or gas. DM subhalos, either massive enough or close enough to the Earth, could be visible in the gamma-ray band [42,43]. More specifically, if 40 GeV DM particles annihilate with a cross section near the latest upper limit, Fermi-LAT might have recorded ∼10 DM subhalos [44–49]. Because of the shortage of stars and gas, DM subhalos may be only detectable in gamma rays and hence are members of the unidentified gamma-ray sources. Dedicated efforts have been made to search for such objects [46–59]. For instance, by fitting spectral energy distribution (SED) with DM spectra, bright high latitude point sources are investigated in [46–49,56]. Candidates are selected from the spectrally hard sources and their multiwavelength counterparts are examined in [51,54]. Independent source candidates created with looser assumptions on the spectrum are studied in [52]. Machine learning algorithms are also used to classify unassociated sources, and outliers, which are probably DM subhalos, are selected [50,53,57]. One very attractive finding is the identification of a spatially extended source, 3FGL J2212.5+0703, among the unidentified sources [48,56] in the Fermi-LAT third source catalog (3FGL). In astrophysical scenarios it is rather hard to give rise to a spatially extended steady source without any association in another wavelength. Therefore, 3FGL J2212.5+0703 is an interesting DM subhalo candidate, as stressed in [56].

Independent analysis is thus necessary to check whether it is indeed the case. For such a purpose, in this work we reanalyze the spatial, temporal, and spectral characters of 3FGL J2212.5+0703. The difference between this work and [48,56] are the following: (1) In order to effectively suppress the possible contamination from two nearby extremely bright blazars (3FGL J2254.0 + 1608 and 3FGL J2232.5 + 1143), we just take into account the front-converting gamma rays that have angular resolutions better than the back-converting photons. (2) We have extended the spectrum analysis down to the energy ∼100 MeV and special attention has been given to the possible improvement in the fit by introducing a phenomenological shape in comparison to the $b\bar{b}$ model. Note that if significant improvement is found, the astrophysical origin will be favored. (3) The variability of the emission in the past eight years rather than just the first four years has been thoroughly examined to better test the stability.

II. OBSERVATION AND DATA ANALYSIS

Fermi-LAT Pass 8 is the most recent iteration of the event-level analysis, which reduces the ghost events (thus leading to an increased effective area and a better point-spread function), extends the energy reach, and introduces new event-type partitions [60]. In this work, we use the front-converting Pass 8 Source data set[1] (irfs=P8R2_SOURCE_V6, evtype=1) and the up-to-date Fermi ScienceTools.[2] We select the data from October 27, 2008 to June 15, 2016 [i.e., mission elapsed time (MET) range 246823875–487641604], and restrict the energy range from 100 MeV to 500 GeV. To avoid significant contamination from the Earth's albedo, photons with zenith angle greater than 90° are excluded. Quality-filter cuts (DATA_QUAL==1 && LAT_CONFIG==1) are also applied so as to remove the events and time intervals while the instrument is not in science configuration, or when either bright solar flares or particle events occur.[3] We consider the photons within a $21° \times 21°$ box centered on the position ($\alpha_{2000} = 333°.147$, $\delta_{2000} = 7°.0598$ [61]) so as to include at least 95% photons[4] of 3FGL J2212.5+0703 at 100 MeV. In order to perform binned analyses, photons are divided into 210×210 spatial bins and 30 logarithmic energy bins.

With the help of the user-contributed script make3FGLxml.py,[5] all 3FGL sources within 25° from the target source [61] as well as the Galactic diffuse γ-ray emission model `gll_iem_v06.fits` and the isotropic emission template for the front-converting source data selection `iso_P8R2_SOURCE_V6_FRONT_v06.txt`[6] [62] are included in the fit. We leave free the spectra of the sources within 10° around 3FGL J2212.5+0703, and the normalizations of the two diffuse emission backgrounds. Note that one of the brightest blazars in the γ-ray band, 3FGL J2254.0 + 1608 (3C 454.3), is at the edge of the region of interest (ROI), whose influence is too significant to be ignored. Therefore, we leave its spectral parameters free, even though it is outside the 10° radius circle. We convolve all these models with the instrument response functions (IRFs) using gtsrcmaps, and then perform the fittings with the pyLikelihood code utilizing the MINUIT algorithm [63]. As recommended in the Fermi Science Center,[7] we take into

[1] ftp://legacy.gsfc.nasa.gov/fermi/data/lat/weekly/photon/.
[2] Version v10r0p5, available at http://fermi.gsfc.nasa.gov/ssc/data/analysis/software/.
[3] http://fermi.gsfc.nasa.gov/ssc/data/analysis/documentation/Cicerone/Cicerone_Data_Exploration/Data_preparation.html.
[4] http://www.slac.stanford.edu/exp/glast/groups/canda/lat_Performance.htm.
[5] http://fermi.gsfc.nasa.gov/ssc/data/analysis/user/.
[6] http://fermi.gsfc.nasa.gov/ssc/data/access/lat/BackgroundModels.html.
[7] http://fermi.gsfc.nasa.gov/ssc/data/analysis/LAT_caveats.html.

TABLE I. The optimized positions and the corresponding TS values of the target source (modeled with a point-source template) and the newly added point sources within 10° from the ROI center.

Source Name	R.A.(°)	Decl.(°)	TS
3FGL J2212.5 + 0703 (pts)	333.13	7.06	320.2
newpt0	327.22	−1.33	25.9
newpt1	329.05	−0.61	146.7
newpt2	332.77	−0.06	36.3

account the energy dispersion of all free sources except the two diffuse emission models.

To check whether there is any significant residual in the ROI, we utilize the gttsmap tool to generate test statistic (TS) maps, which are shown in Fig. 1. The TS is defined as $-2\ln(\mathcal{L}_{\max,0}/\mathcal{L}_{\max,1})$ [64], where $\mathcal{L}_{\max,1}$ and $\mathcal{L}_{\max,0}$ are the best-fit likelihood values of the alternative hypothesis (i.e., include a point source) and null hypothesis (i.e., background only), respectively. We make a $20° \times 20°$ TS map and find three new point sources within 10° distance from the ROI center with a TS value larger than 25. We first add these new point sources into the model with power-law spectra and coarse locations derived from the TS map, then do a fitting with energy dispersion turned off. Using that fitted model as an input, the positions of these point sources as well as the target source 3FGL J2212.5+0703 are optimized with gtfindsrc. With the best-fit positions, we further fit the spectra with energy dispersion enabled and the results are summarized in Table I.

Note that our spectral parameters of the center source are in agreement with the values listed in the 3FGL catalog (within the 2σ confidence level). Moreover, there is almost no shift in position for 3FGL J2212.5+0703.

A. Spatial extension

Spatial extension is an important property for a source. As argued in [56], an unambiguously spatially extended source without multiwavelength associations could be a nearby DM subhalo. In the left panel of Fig. 1, some residuals remain near 3FGL J2212.5+0703 when we model it with a point-source template. To get a quick insight into the morphology of 3FGL J2212.5+0703, we exclude it from the model and calculate the TS map again. The TS map is exhibited in the right panel of Fig. 1. 3FGL J2212.5+0703 appears elliptical in TS map, and the residual in the left panel of Fig. 1 is caused by the incorrect spatial template.

Following [48], to quantify the spatial extension we use a series of 2D Gaussian distributions with different widths σ as spatial templates. Based on the optimized model in the previous subsection, we change the spatial template and perform optimizations. The same likelihood ratio test is applied to achieve the best-fit spatial extension and the corresponding significance. We define the TS for spatial extension to be

$$\mathrm{TS}_{\mathrm{ext}} = -2\ln\left(\frac{\mathcal{L}_{\mathrm{point}}}{\mathcal{L}_{\mathrm{ext}}}\right), \tag{1}$$

where $\mathcal{L}_{\mathrm{point}}$ and $\mathcal{L}_{\mathrm{ext}}$ are the best-fit likelihood values for the point-source model and the Gaussian model, respectively [65]. Figure 2 depicts the relation between the widths and the TS values. We find that the Gaussian template with

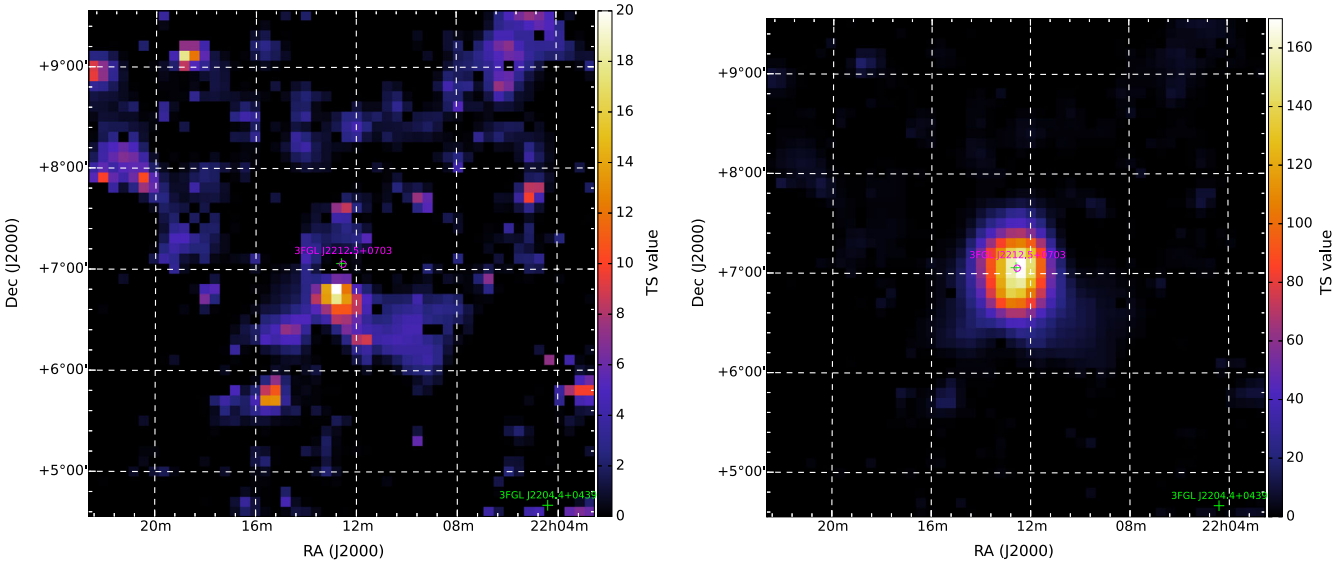

FIG. 1. $5° \times 5°$ TS maps of the 3FGL J2212.5 + 0703 region using the front-converting Pass 8 data in the energy range of 1–500 GeV. We show the TS map with (without) target source included in the model in the left (right) panel. The green cross in the center of the figure is the position of target source listed in the catalog, while the magenta circle shows the position fitted with gtfindsrc.

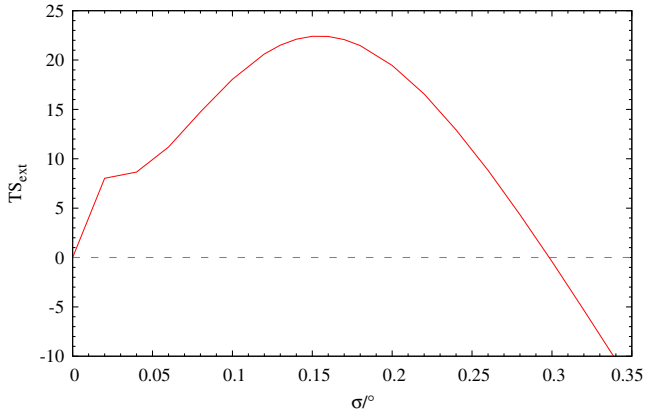

FIG. 2. The increase in the TS value of 3FGL J2212.5 + 0703 when a Gaussian template instead of a point-like one is incorporated in the data fit. The best-fit template is the one with a width of 0°.15 and the corresponding TS_{ext} is 22.4.

a width of 0°.15 best describes the data and the corresponding TS_{ext} value is 22.4, implying that the spatial-extended source model is better than the point-source model at a confidence level of $\sim 4.7\sigma$ [65,66]. Such an improvement is smaller than that reported in [56] since in this work different spatial templates are used and just the front-converting Pass 8 data have been taken into account.

B. The light curve and variability

The γ-ray signal from DM annihilation in a subhalo should be steady while the astrophysical signal may be variable. With approximately four more years of data compared with 3FGL [61], we can better test the compatibility of 3FGL J2212.5+0703 with a nonvariable source. The data are separated into 16 time bins equally. We use the best-fit Gaussian template, and set free the normalization of the isotropic emission as well as the prefactors of the sources within 10° around 3FGL J2212.5+0703. To better model the nearby bright blazars, 3FGL J2254.0 + 1608 and 3FGL J2232.5 + 1143, we free both the normalizations and the indexes of them. A fitting is performed in each time bin, and the likelihood profile of the target source is calculated.

The flux in each time bin is computed and the light curve of 3FGL J2212.5+0703 is yielded, as shown in Fig. 3. The variability index is defined as [67]

$$\mathrm{TS}_{\mathrm{var}} = -2\sum_{\mathrm{i}} \frac{\Delta F_{\mathrm{i}}^2}{\Delta F_{\mathrm{i}}^2 + f^2 F_{\mathrm{const}}^2} \ln\left(\frac{\mathcal{L}_{\mathrm{i}}(F_{\mathrm{const}})}{\mathcal{L}_{\mathrm{i}}(F_{\mathrm{i}})}\right), \quad (2)$$

where for the ith time bin, $\mathcal{L}_{\mathrm{i}}$ is the likelihood value, F_{i} is the photon flux integrated over the energy range from 100 MeV to 500 GeV, and ΔF_{i} is the statistical uncertainty[8] of the flux F_{i}. F_{const} is the flux if the source is constant, and f is the systematic correction factor. Following [61] we also

[8]We use the upper error of the flux.

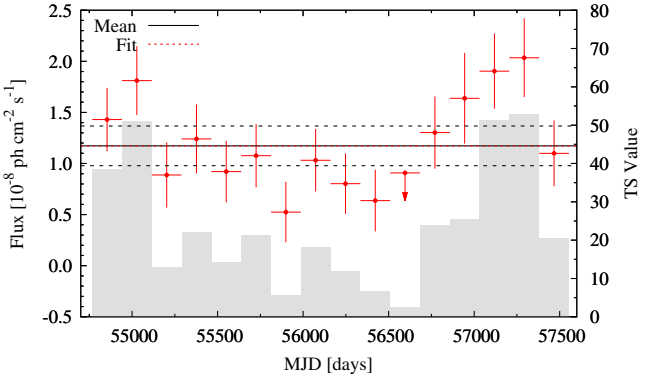

FIG. 3. The light curve of 3FGL J2212.5 + 0703. Red points are the fluxes integrated from 100 MeV to 500 GeV, while the TS value of each time interval is shown in gray histogram. 95% upper limits are drawn when the TS values are smaller than 5. The solid line and two dashed horizontal lines represent the average flux and its 1σ range, respectively. The dotted line is the flux derived from the fit of the flux-likelihood relation in different time bins, which is almost the same as the average flux. In this analysis, we find the variability index to be 33.2 with 15 degrees of freedom, indicating no significant ($\sim 2.6\sigma$) deviation from being a steady source.

take into account a 2% systematic correction factor. Using the likelihood profile we fit F_{const} in the above expression. The variability index is found to be 33.2 after the optimization, which corresponds to a significance of $\sim 2.6\sigma$ for the deviation from the nonvariable hypothesis, for an approximate χ^2 distribution with 15 degrees of freedom [68]. The variability at time scales shorter than 6 months may not be effectively reflected in the above analysis, so we further do similar calculation using the data with one-month's time bin. To make the fitting stable, we fix the indexes of the two blazars mentioned above. The variability index is found to be 123.2, corresponding to a $\sim 2.1\sigma$ significance for 92 degrees of freedom.

C. Spectral analysis

The γ rays from DM annihilation are characterized by a hard low-energy spectrum and a sharp cutoff at the mass of the DM particle, so it is possible to distinguish between the DM model and the astrophysical origin model with the spectral information. If an "astrophysical" spectrum model can significantly better fit the gamma-ray data than the DM one, and meanwhile give a flat spectrum in low-energy range, a DM origin would be disfavored. We compute the SED of 3FGL J2212.5+0703 to illustrate the spectrum in a model-independent way. The data are binned with 15 equal logarithmic energy bins within the energy range from 100 MeV to 100 GeV. We set the indexes of all sources frozen, and optimize their normalizations in each energy bin. The intensity and TS value in each energy bin are shown in Fig. 4. According to the derived SED, we find that the spectrum of the target source is curved and can be well

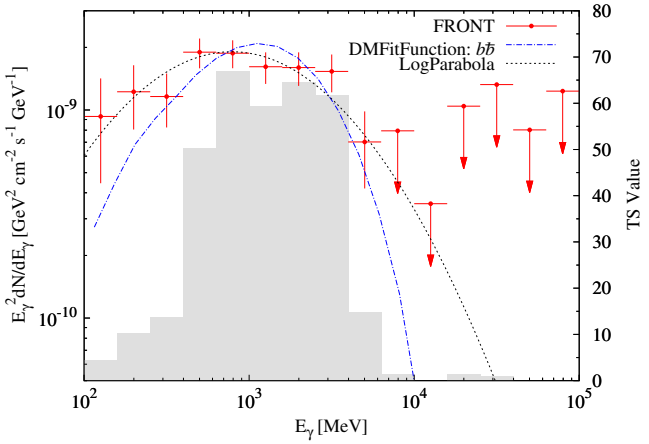

FIG. 4. The spectral energy distribution (SED) of 3FGL J2212.5 + 0703 and two types of spectral modeling. Gray histograms represent the TS values in different energy bins. We use two types of spectra to fit the data, i.e., the generic LogParabola spectrum and the DMFitFunction spectrum which predicts the annihilation of 18.5 GeV DM particles to $b\bar{b}$, and the corresponding spectra are shown in black (dashed) line and blue (dotted dashed) line, respectively. The TS value difference between these two models is 7.0, implying that both models works almost equally well.

described by a LogParabola spectrum, which is the phenomenological model given in the catalog. The DM spectrum model can well fit the data too (the spectrum might be a bit softer than the $b\bar{b}$ model at energies below 300 MeV. The error bars however are too large).

In order to compare the two spectral models quantitatively, we fit the data from 100 MeV to 500 GeV using the DMFitFunction with the primary decay channel $b\bar{b}$ and the LogParabola model,[9] respectively. The optimized spectra obtained in these fittings are also plotted in Fig. 4. In the DM model, observational data favor a DM particle with a mass of 18.5 GeV. Considering the probability function of the DM mass may not be a Gaussian distribution, we make a likelihood profile to find a more accurate 1σ confidence interval (CI) of DM mass. We use a series of DM annihilation spectra from different DM masses, and do the fittings. The edges of the 1σ CI correspond to the models where the log-likelihood is 0.5 smaller than the maximum one [69]. We find the 1σ CI of DM mass to be (15.7, 20.9) GeV.[10] We note the CI is different from that in [56], which is due to the different spatial morphology and analysis method. The spectral TS,

$$\mathrm{TS}_{\mathrm{spec}} = -2\ln\left(\frac{\mathcal{L}_{b\bar{b}}}{\mathcal{L}_{\log\,\mathrm{p}}}\right), \tag{3}$$

is calculated, where $\mathcal{L}_{\log\,\mathrm{p}}$ and $\mathcal{L}_{b\bar{b}}$ are maximum likelihood values for the LogParabola model and the DMFitFunction model, respectively. Through the fit, we find $\mathrm{TS}_{\mathrm{spec}}$ to be 7.0, which indicates the LogParabola model is more compatible with the data. Please bear in mind that the two spectral models are not nested in parameter space, so a significance can not be obtained from the Wilks theorem [68]. Since the TS value is quite small, the preference of the LogParabola model is weak. More data are needed to draw a better conclusion.

III. DISCUSSION AND CONCLUSION

DM subhalos are interesting targets for dark matter indirect detection. In principle some DM subhalos with little stars and dust may be only detectable in gamma rays and are thus members of unidentified gamma-ray sources. After the successful performance of Fermi-LAT, great efforts have been made to identify such sources and one very attractive finding is the identification of a spatially extended source, 3FGL J2212.5+0703, among the unidentified sources [48,56] in the Fermi-LAT 3FGL. Usually, the astrophysical processes are hard to give rise to a spatially extended steady source without any signals in other bands. Therefore 3FGL J2212.5+0703 is an interesting DM subhalo candidate, as stressed in [56]. Extended and independent analysis is necessary to check whether it is indeed the case. In this work we reanalyze the spatial, temporal, and spectral characteristics of 3FGL J2212.5+0703. In order to effectively reduce the possible contamination from two nearby extremely bright blazars (3FGL J2254.0 + 1608 and 3FGL J2232.5 + 1143), just the front-converting gamma rays (with better angular resolutions than the back-converting photons) have been taken into account. With such data we confirm that 3FGL J2212.5+0703 is indeed a spatially extended source rather than a point source and the optimized template has a width of 0°.15. We have also extended the spectrum analysis down to the energy ~100 MeV and the main goal is to test whether an astrophysical spectrum model (i.e., the phenomenological LogParabola model) can significantly better fit the gamma-ray data than the simple DM $b\bar{b}$ channel model. No significant improvement is found (the increase in TS is just ~7), implying that both the astrophysical model and the DM model (with a rest mass $m_\chi \sim 20$ GeV) work almost equally well. In principle, the spectral model can be better constrained as more data have been collected in the future. However, it is unlikely that the Fermi-LAT data for 3FGL J2212.5+0703 can be doubled. Even for the doubled gamma-ray data, it seems still challenging to distinguish between the two types of spectral models. Finally, we checked the possible variability in the

[9]We use the table gammamc_dif.dat, which is required in DMFitFunction, contained in the FermiPy package. FermiPy can be downloaded from https://github.com/fermiPy/fermipy.

[10]We also use the DM spectra from the PPPC4 [70] and make the likelihood profile. We find the best-fit mass is about 20.0 GeV and the 1σ CI is (17.8, 23.2) GeV.

~8 years' data and did not find significant evidence for deviation from a constant flux.

If 3FGL J2212.5+0703 is indeed a DM subhalo, its parameters cannot be too extreme compared with those in N-body simulations. Since the flux of the optimized DM model (with a rest mass $m_\chi = 18.5$ GeV) from 100 MeV to 500 GeV is $(8.2 \pm 0.6) \times 10^{-9}$ ph cm^{-2} s^{-1}, if the velocity-averaged annihilation cross section of DM particles is assumed to be $\langle \sigma v \rangle = 2 \times 10^{-26}$ cm^3 s^{-1}, we can derive that $\int_{V_{\rm sub}} \rho^2_{\rm sub}(\boldsymbol{x}) d^3\boldsymbol{x}/(M^2_\odot {\rm pc}^{-3}) = (4.7 \pm 0.3) \times 10^4 (D/{\rm kpc})^2$, where $\rho_{\rm sub}$ is the mass density of the subhalo and D is the distance between the Sun and the source. Referring to clump luminosity-distance plane shown in Fig. 2 of Brun *et al.* [71], we find the target source is near the median distances calculated from a random sample of observer positions. Therefore, a DM subhalo origin is not challenged.

Our conclusion is thus 3FGL J2212.5+0703 is indeed a steady spatially extended unidentified gamma-ray source. These remarkable characteristics are compatible with the gamma-ray signal from a self-annihilating DM subhalo though how to yield such bright emission is still to be figured out. The other possibility that 3FGL J2212.5+0703 actually consists of two or more very nearby γ-ray sources also deserves a further investigation. More γ-ray data as well as deeper multiwavelength observations are needed to draw a final conclusion.

ACKNOWLEDGMENTS

We would like to thank Dr. X. Li for useful discussions. This research has made use of data obtained from the High Energy Astrophysics Science Archive Research Center (HEASARC), provided by NASA Goddard Space Flight Center. This research has also used IPython [72], NumPy, SciPy [73], Matplotlib [74], `Astropy` [75], `F2PY` [76], APLpy[11] and `iminuit`.[12] This work was supported in part by the National Basic Research Program of China (No. 2013CB837000) and the National Key Program for Research and Development (No. 2016YFA0400200), the National Natural Science Foundation of China under Grants No. 11525313 (that is the Funds for Distinguished Young Scholars), No. 11103084, No. 11303098 and No. 11303105, and the 100 Talents program of Chinese Academy of Sciences.

[11] http://aplpy.github.com.
[12] https://github.com/iminuit/iminuit.

[1] G. Jungman, M. Kamionkowski, and K. Griest, Phys. Rep. **267**, 195 (1996).
[2] G. Bertone, D. Hooper, and J. Silk, Phys. Rep. **405**, 279 (2005).
[3] G. Bertone and D. Hooper, arXiv:1605.04909.
[4] P. A. R. Ade *et al.* (Planck Collaboration), Astron. Astrophys. **594**, A13 (2016).
[5] D. Hooper and S. Profumo, Phys. Rep. **453**, 29 (2007).
[6] J. L. Feng, Annu. Rev. Astron. Astrophys. **48**, 495 (2010).
[7] E. Charles *et al.*, Phys. Rep. **636**, 1 (2016).
[8] W. Atwood *et al.* (Fermi-LAT Collaboration), Astrophys. J. **697**, 1071 (2009).
[9] D. G. York *et al.* (SDSS Collaboration), Astron. J. **120**, 1579 (2000).
[10] A. W. McConnachie, Astron. J. **144**, 4 (2012).
[11] K. Bechtol, A. Drlica-Wagner *et al.* (DES Collaboration), Astrophys. J. **807**, 50 (2015).
[12] A. Drlica-Wagner, K. Bechtol *et al.* (DES Collaboration), Astrophys. J. **813**, 109 (2015).
[13] S. E. Koposov, V. Belokurov, G. Torrealba, and N. Wyn Evans, Astrophys. J. **805**, 130 (2015).
[14] D. Kim and H. Jerjen, Astrophys. J. Lett. **808**, L39 (2015).
[15] B. P. M. Laevens, N. F. Martin, R. A. Ibata *et al.*, Astrophys. J. Lett. **802**, L18 (2015).
[16] B. P. M. Laevens, N. F. Martin *et al.*, Astrophys. J. **813**, 44 (2015).
[17] N. F. Martin, D. L. Nidever *et al.*, Astrophys. J. Lett. **804**, L5 (2015).
[18] D. Kim, H. Jerjen, D. Mackey, G. S. Da Costa, and A. P. Milone, Astrophys. J. Lett. **804**, L44 (2015).
[19] T. Abbott *et al.* (DES Collaboration), arXiv:astro-ph/0510346.
[20] N. Kaiser *et al.*, *Proc. SPIE Int. Soc. Opt. Eng.* 4836, 154 (2002).
[21] A. A. Abdo *et al.* (Fermi-LAT Collaboration), Astrophys. J. **712**, 147 (2010).
[22] M. Ackermann *et al.* (Fermi-LAT Collaboration), Phys. Rev. Lett. **107**, 241302 (2011).
[23] A. Geringer-Sameth and S. M. Koushiappas, Phys. Rev. Lett. **107**, 241303 (2011).
[24] Y.-L. S. Tsai, Q. Yuan, and X. Huang, J. Cosmol. Astropart. Phys. 03 (2013) 018.
[25] M. N. Mazziotta, F. Loparco, F. de Palma, and N. Giglietto, Astropart. Phys. **37**, 26 (2012).
[26] I. Cholis and P. Salucci, Phys. Rev. D **86**, 023528 (2012).
[27] M. Ackermann *et al.* (Fermi-LAT Collaboration), Phys. Rev. D **89**, 042001 (2014).
[28] A. Geringer-Sameth, S. M. Koushiappas, and M. G. Walker, Phys. Rev. D **91**, 083535 (2015).
[29] A. Geringer-Sameth, M. G. Walker, S. M. Koushiappas, S. E. Koposov, V. Belokurov, G. Torrealba, and N. Wyn Evans, Phys. Rev. Lett. **115**, 081101 (2015).

[30] A. Drlica-Wagner, A. Albert *et al.* (Fermi-LAT Collaboration), Astrophys. J. Lett. **809**, L4 (2015).
[31] M. Ackermann *et al.* (Fermi-LAT Collaboration), Phys. Rev. Lett. **115**, 231301 (2015).
[32] D. Hooper and T. Linden, J. Cosmol. Astropart. Phys. 09 (2015) 016.
[33] M. G. Baring, T. Ghosh, F. S. Queiroz, and K. Sinha, Phys. Rev. D **93**, 103009 (2016).
[34] S. Li, Y.-F. Liang, K.-K. Duan, Z.-Q. Shen, X. Huang, X. Li, Y.-Z. Fan, N.-H. Liao, L. Feng, and J. Chang, Phys. Rev. D **93**, 043518 (2016).
[35] M. L. Ahnen *et al.* (MAGIC Collaboration), J. Cosmol. Astropart. Phys. 02 (2016) 039.
[36] Y.-F. Liang, Z.-Q. Xia, Z.-Q. Shen, X. Li, W. Jiang, Q. Yuan, Y.-Z. Fan, L. Feng, E.-W. Liang, and J. Chang, Phys. Rev. D **94**, 103502 (2016).
[37] A. Albert *et al.* (Fermi-LAT Collaboration and DES Collaboration), arXiv:1611.03184.
[38] S. D. M. White and M. J. Rees, Mon. Not. R. Astron. Soc. **183**, 341 (1978).
[39] S. D. M. White and C. S. Frenk, Astrophys. J. **379**, 52 (1991).
[40] J. Diemand, M. Kuhlen, and P. Madau, Astrophys. J. **657**, 262 (2007).
[41] V. Springel, J. Wang, M. Vogelsberger, A. Ludlow, A. Jenkins, A. Helmi, J. F. Navarro, C. S. Frenk, and S. D. M. White, Mon. Not. R. Astron. Soc. **391**, 1685 (2008).
[42] V. Springel, S. D. M. White, C. S. Frenk, J. F. Navarro, A. Jenkins, M. Vogelsberger, J. Wang, A. Ludlow, and A. Helmi, Nature (London) **456**, 73 (2008).
[43] Q. Yuan, Y. Cao, J. Liu, P.-F. Yin, L. Gao, X.-J. Bi, and X. Zhang, Phys. Rev. D **86**, 103531 (2012).
[44] M. Kuhlen, J. Diemand, and P. Madau, Astrophys. J. **686**, 262 (2008).
[45] B. Anderson, M. Kuhlen, J. Diemand, R. P. Johnson, and P. Madau, Astrophys. J. **718**, 899 (2010).
[46] M. R. Buckley and D. Hooper, Phys. Rev. D **82**, 063501 (2010).
[47] A. V. Belikov, M. R. Buckley, and D. Hooper, Phys. Rev. D **86**, 043504 (2012).
[48] B. Bertoni, D. Hooper, and T. Linden, J. Cosmol. Astropart. Phys. 12 (2015) 035.
[49] D. Schoonenberg, J. Gaskins, G. Bertone, and J. Diemand, J. Cosmol. Astropart. Phys. 05 (2016) 028.
[50] N. Mirabal, D. Nieto, and S. Pardo, arXiv:1007.2644.
[51] H.-S. Zechlin, M. V. Fernandes, D. Elsässer, and D. Horns, Astron. Astrophys. **538**, A93 (2012).
[52] M. Ackermann *et al.* (Fermi-LAT Collaboration), Astrophys. J. **747**, 121 (2012).
[53] N. Mirabal, V. Frias-Martinez, T. Hassan, and E. Frías-Martinez, Mon. Not. R. Astron. Soc. **424**, L64 (2012).
[54] H.-S. Zechlin and D. Horns, J. Cosmol. Astropart. Phys. 11 (2012) 050.
[55] A. Berlin and D. Hooper, Phys. Rev. D **89**, 016014 (2014).
[56] B. Bertoni, D. Hooper, and T. Linden, J. Cosmol. Astropart. Phys. 05 (2016) 049.
[57] N. Mirabal, E. Charles, E. C. Ferrara, P. L. Gonthier, A. K. Harding, M. A. Sánchez-Conde, and D. J. Thompson, Astrophys. J. **825**, 69 (2016).
[58] D. Hooper and S. J. Witte, arXiv:1610.07587.
[59] Z.-Q. Xia, K.-K. Duan, S. Li, Y.-F. Liang, Z.-Q. Shen, C. Yue, Y.-P. Wang, Q. Yuan, Y.-Z. Fan, J. Wu, and J. Chang, arXiv:1611.05565.
[60] W. Atwood *et al.* (Fermi-LAT Collaboration), arXiv:1303.3514.
[61] F. Acero *et al.* (Fermi-LAT Collaboration), Astrophys. J. Suppl. Ser. **218**, 23 (2015).
[62] F. Acero *et al.* (Fermi-LAT Collaboration), Astrophys. J. Suppl. Ser. **223**, 26 (2016).
[63] F. James and M. Roos, Comput. Phys. Commun. **10**, 343 (1975).
[64] J. R. Mattox, D. L. Bertsch *et al.*, Astrophys. J. **461**, 396 (1996).
[65] J. Lande, M. Ackermann *et al.*, Astrophys. J. **756**, 5 (2012).
[66] H. Chernoff, Ann. Math. Stat. **25**, 573 (1954).
[67] P. L. Nolan *et al.* (Fermi-LAT Collaboration), Astrophys. J. Suppl. Ser. **199**, 31 (2012).
[68] S. S. Wilks, Ann. Math. Stat. **9**, 60 (1938).
[69] J. Conrad, Astropart. Phys. **62**, 165 (2015).
[70] M. Cirelli, G. Corcella, A. Hektor, G. Hütsi, M. Kadastik, P. Panci, M. Raidal, F. Sala, and A. Strumia, J. Cosmol. Astropart. Phys. 03 (2011) 051.
[71] P. Brun, T. Delahaye, J. Diemand, S. Profumo, and P. Salati, Phys. Rev. D **80**, 035023 (2009).
[72] F. Perez and B. E. Granger, Comput. Sci. Eng. **9**, 21 (2007).
[73] S. van der Walt, S. C. Colbert, and G. Varoquaux, Comput. Sci. Eng. **13**, 22 (2011).
[74] J. D. Hunter, Comput. Sci. Eng. **9**, 90 (2007).
[75] T. P. Robitaille *et al.*, Astron. Astrophys. **558**, A33 (2013).
[76] P. Peterson, Int. J. Comput. Sci. Eng. **4**, 296 (2009).